nature biotechnology

Suppression of vascular permeability and inflammation by targeting of the transcription factor c-Jun

Roger G Fahmy[1], Alla Waldman[1], Guishui Zhang[1], Ainslie Mitchell[1], Nicodemus Tedla[2], Hong Cai[2], Carolyn R Geczy[2], Colin N Chesterman[1], Michael Perry[3] & Levon M Khachigian[1]

Conventional anti-inflammatory strategies induce multiple side effects, highlighting the need for novel targeted therapies. Here we show that knockdown of the basic-region leucine zipper protein, c-Jun, by a catalytic DNA molecule, Dz13, suppresses vascular permeability and transendothelial emigration of leukocytes in murine models of vascular permeability, inflammation, acute inflammation and rheumatoid arthritis. Treatment with Dz13 reduced vascular permeability due to cutaneous anaphylactic challenge or VEGF administration in mice. Dz13 also abrogated monocyte-endothelial cell adhesion *in vitro* and abolished leukocyte rolling, adhesion and extravasation in a rat model of inflammation. Dz13 suppressed neutrophil infiltration in the lungs of mice challenged with endotoxin, a model of acute inflammation. Finally, Dz13 reduced joint swelling, inflammatory cell infiltration and bone erosion in a mouse model of rheumatoid arthritis. Mechanistic studies showed that Dz13 blocks cytokine-inducible endothelial c-Jun, E-selectin, ICAM-1, VCAM-1 and VE-cadherin expression but has no effect on JAM-1, PECAM-1, p-JNK-1 or c-Fos. These findings implicate c-Jun as a useful target for anti-inflammatory therapies.

The efficacy of conventional anti-inflammatory treatments has been limited by collateral effects such as obesity, gastrointestinal toxicity, immunosuppression, bleeding and cardiovascular morbidity[1–4]. Inflammation[5] and angiogenesis[6] both depend on increased vascular permeability. Loosening of established endothelial cell-cell contacts is necessary for leukocyte emigration from the circulation into the subendothelial space and for blood vessel sprouting from the pre-existing vasculature. The precise mechanisms underlying these processes are incompletely understood, although vascular endothelial growth factor (VEGF)[7], the angiopoietins[8], the angiopoietin-related proteins[9] and Akt1[10] are among the key players. Much less is known about the nuclear transcription factors involved. As drivers of gene expression, transcription factors may prove particularly efficacious as upstream therapeutic targets. Previously we have targeted transcription factors to inhibit intimal thickening in injured rat carotid arteries[11–13] and in-stent restenosis in injured pig coronary arteries[14]. More recently we have shown that targeting of c-Jun, a basic-region leucine zipper protein and AP1 family member, inhibits microvascular endothelial cell proliferation, migration, invasion and microtubule formation *in vitro*[15] and suppresses VEGF-induced neovascularization *in vivo*[15]. Based on these results, we hypothesized that c-Jun targeting may suppress vascular permeability and inflammation, ultimately providing an alternative strategy to conventional anti-inflammatory treatments, such as steroids, nonsteroidal anti-inflammatory drugs and steroid-sparing agents, which each have limitations[1,3,4].

We targeted c-Jun with a catalytic DNA molecule, Dz13 (ref. 13), a 34-bp oligonucleotide that cleaves murine c-Jun mRNA at G^{967} (or G^{1311} in human c-Jun mRNA). A 3′-3′ inverted thymidine linkage in Dz13 confers improved stability against nuclease degradation[11].

Exposure of neonatal mice to hyperoxic conditions followed by normoxia results in retinal neovascularization[16] (**Fig. 1a**). Single intravitreal administration of Dz13 (20 μg) inhibited retinal neovascularization compared with mice treated with an identical amount of the control DNAzyme, Dz13scr. Dz13scr retains the 15-nt catalytic domain of Dz13 but its hybridizing arms are scrambled (**Fig. 1a**); Dz13scr has identical size, net charge, base composition to Dz13 but is unable to cleave c-Jun mRNA[13]. Retinal neovascularization was also inhibited by intravitreal delivery of a synthetic siRNA targeting c-Jun but not by siRNAscr (**Fig. 1a**). The sequences targeted by Dz13 and the siRNA in the murine c-Jun mRNA (NM_010591) are separated by ~1.5 kb (Dz13 targets nucleotides (nts) 958–976, whereas the siRNA targets nts 2465–2485). Fluorescence microscopy following administration of the DNAzyme or siRNA bearing fluorescein isothiocyanate (FITC) moieties confirmed delivery to the vascular endothelial lining (**Fig. 1a**). No fluorescent signal was detected with either nucleic acid molecule not conjugated with FITC (**Fig. 1a**) thereby excluding artifact caused by autofluorescence.

Next, we studied the effect of c-Jun targeting on vascular permeability using passive cutaneous anaphylaxis in mice. Vascular leakage in this model is detected by Evans blue dye extravasation from the bloodstream into tissue as a consequence of IgE-dinitrophenyl (DNP)/DNP-induced passive cutaneous anaphylaxis (**Fig. 1b**, upper left panel). Local injection of a single dose (100 μg) of Dz13 was sufficient to inhibit the vascular response in the ears of Balb/c mice by 70%

[1]Centre for Vascular Research, University of New South Wales, and Department of Haematology, The Prince of Wales Hospital, Sydney NSW 2031, Australia. [2]Cytokine Research Unit, Department of Pathology, [3]Department of Physiology and Pharmacology, University of New South Wales, Sydney NSW 2052, Australia. Correspondence should be addressed to L.M.K. (l.khachigian@unsw.edu.au).

Received 12 January; accepted 26 May; published online 2 July 2006; corrected after print 10 June 2015; doi:10.1038/nbt1225

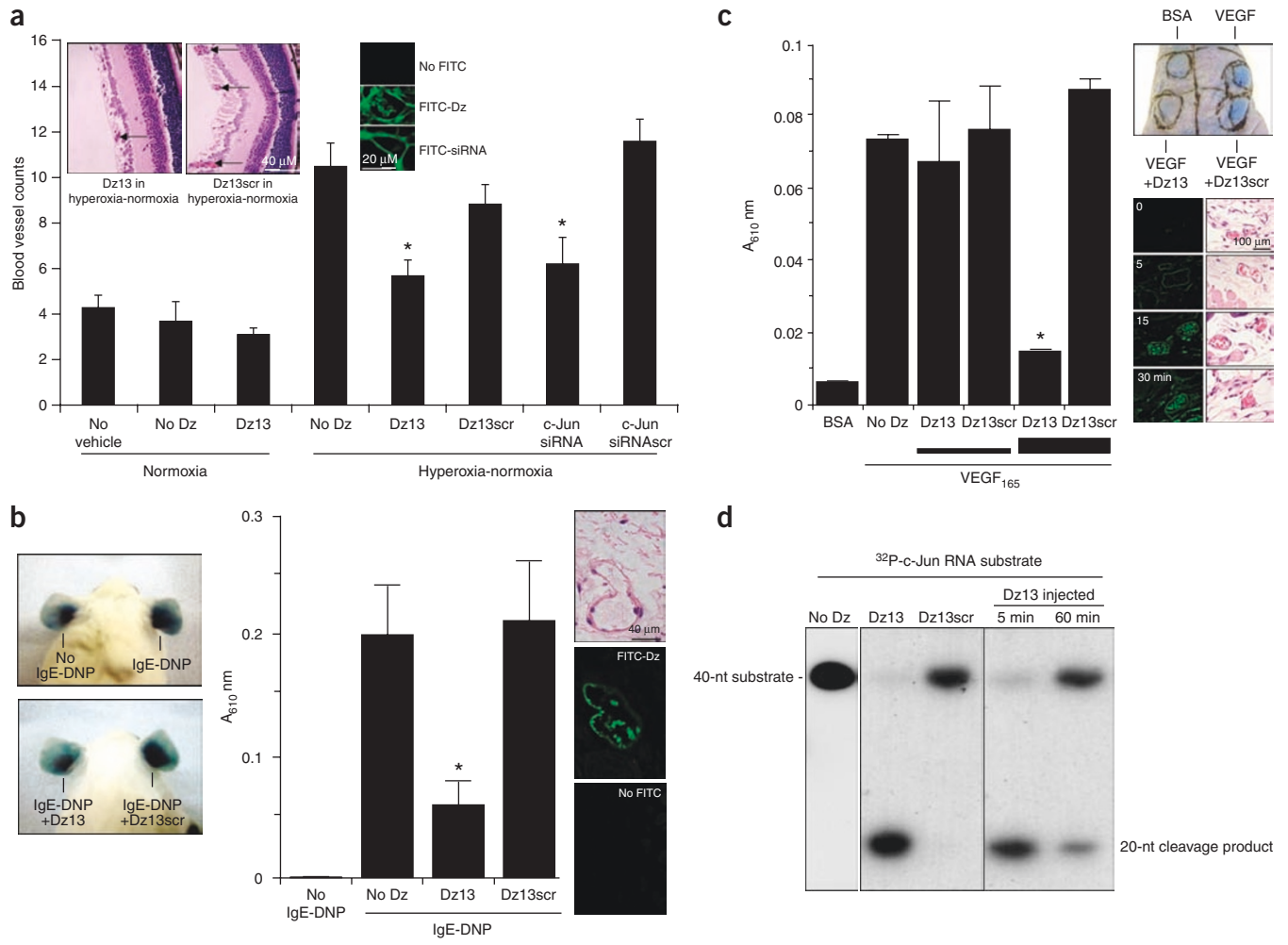

Figure 1 Dz13 localizes to vascular endothelium and inhibits retinal neovascularization and vascular leakiness. (**a**) Dz13 inhibits retinal neovascularization in the retinopathy-of-prematurity model. Serial cross sections of the eyes were stained with H&E and blood vessels in the retina were quantified by light microscopy under 400× magnification and expressed as the mean ± s.e.m. The figure shows localization of FITC-labeled DNAzyme or siRNA in retinal neovessels by fluorescence microscopy. 'No vehicle' represents the normoxia control without vehicle (transfection agent) or DNAzyme or siRNA. All other groups contain vehicle. (**b**) Dz13 inhibits vascular permeability induced by IgE-DNP in the passive cutaneous anaphylaxis model. The figure shows representative dye leakage and localization of FITC-labeled DNAzyme in blood vessels in ears by fluorescence microscopy (with corresponding H&E-stained sister sections shown). (**c**) Dz13 inhibits $VEGF_{165}$-induced vascular permeability in the Miles assay. The figure shows time-dependent tissue accumulation of FITC-labeled DNAzyme and sister H&E-stained cross sections. (**d**) Intradermal injections of 100 μg Dz13 were given to 6-week-old female Balb/c nude mice. At 5 and 60 min, skin surrounding the injection site was resected, homogenized in 1.2 ml TRIzol and DNA extracted from skin tissue and column purified. The DNA was incubated with ^{32}P-5′-end labeled 40-nt RNA substrate (5′-UGCCCUCAACGCCUCGUUCCUCCCGUCCGAGAGCGGACCU-3′) for 1 h at 37 °C. Cleavage products were separated by electrophoresis on 12% PAGE denaturing gels and visualized by autoradiography. Dz13 is the scrambled arm counterpart of Dz13. *, $P < 0.05$ compared to control using Student's *t*-test or ANOVA.

(**Fig. 1b**, lower left and middle panels). In contrast, Dz13scr had no inhibitory effect (**Fig. 1b**, lower left and middle panels). Experiments using FITC-labeled DNAzyme demonstrated localization in endothelium (**Fig. 1b**, right panels).

We further investigated the capacity of Dz13 to inhibit vascular permeability using the Miles assay in athymic Balb/c nude mice. In this model, intradermal administration of $VEGF_{165}$ causes leakage of Evans blue dye from the circulation into tissue. Intradermal injection of $VEGF_{165}$ induced dye leakage within 90 min (**Fig. 1c**). Dye leakage was blocked 80% by prior local administration of a single dose (100 μg) of Dz13, but not Dz13scr (**Fig. 1c**). In contrast, 10 μg of Dz13 in the same volume of vehicle had no effect on dye leakage (**Fig. 1c**) indicating that Dz13 inhibition of vascular permeability is dose dependent. FITC-labeled Dz13 localized to the endothelium and surrounding structures in a time-dependent manner (**Fig. 1c**, lower right panels). DNAzyme Dz14 (ref. 13), which targets nts 1145–1162 (cleavage at A^{1154}) in murine c-Jun mRNA, did not affect dye extravasation in this model (data not shown), consistent with our previous demonstration that Dz14 does not cleave c-Jun mRNA[13]. To demonstrate that Dz13 retained its activity after intradermal injection, we extracted DNA from the skin at various times and added it to a standard *in vitro* cleavage reaction with ^{32}P-labeled 40-nt synthetic RNA substrate. Dz13 was catalytically active 5 min after delivery, and cleavage product was apparent even after 60 min (**Fig. 1d**).

The preceding data showing Dz13 inhibition of vascular leakiness led us to investigate whether c-Jun plays a role in leukocyte infiltration through permeable endothelium. First, using an *in vitro* coculture model, we determined whether c-Jun was required for monocytic cell adhesion. Interleukin (IL)-1beta stimulated THP-1 monocytic cell adhesion to human microvascular endothelial cell (HMEC-1 line)

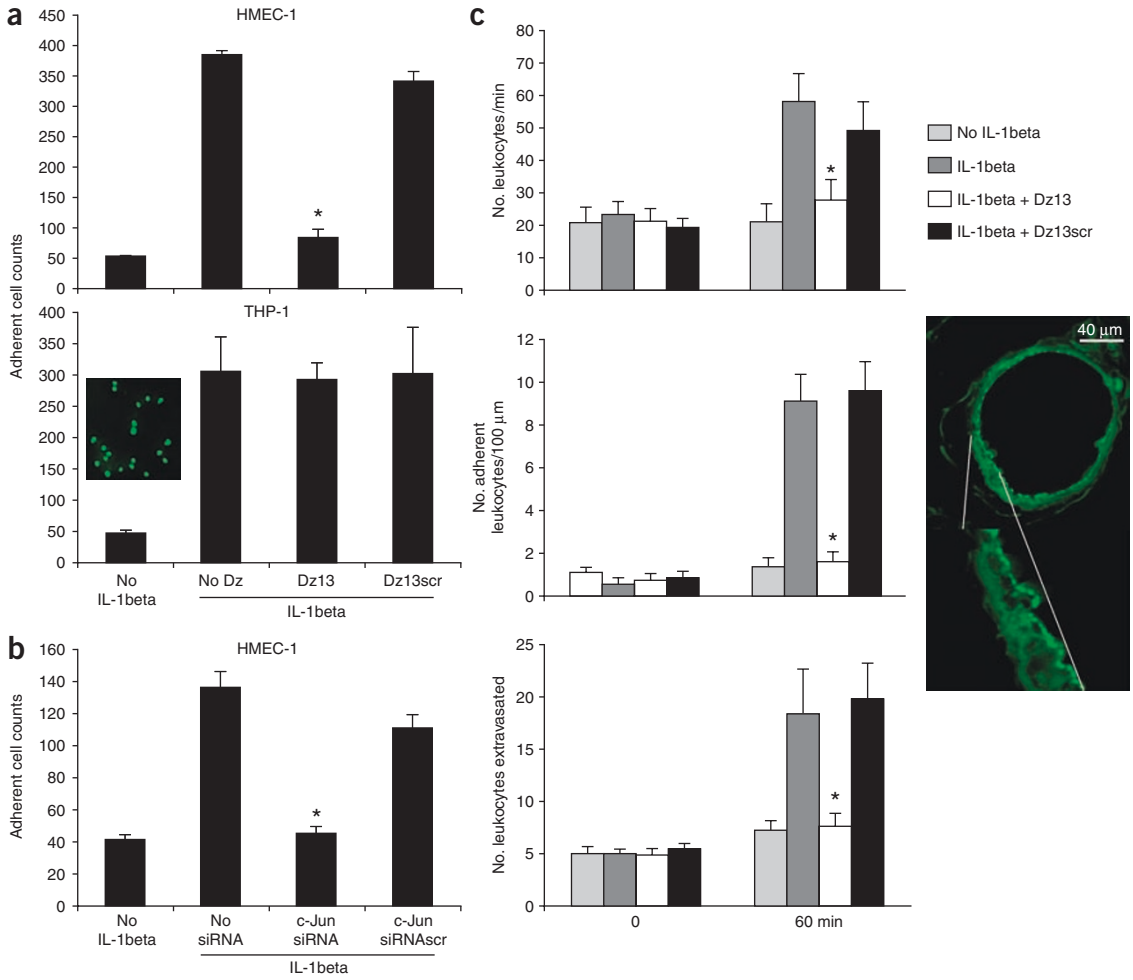

Figure 2 Dz13 inhibits cytokine-inducible monocytic cell–endothelial cell adhesion *in vitro* and inflammation in mesenteric microcirculation of rats. (**a**) HMEC-1 transfected with Dz13 or Dz13scr were incubated with IL-1beta before the addition of a suspension of THP-1 monocytic cells. Alternatively the THP-1 cells were transfected with DNAzyme. Fluorescence microscopy demonstrates that although THP-1 cells took up FITC-labeled DNAzyme, Dz13 failed to inhibit adhesion of the monocytic cells to endothelial cells. (**b**) HMEC-1 transfected with siRNA or siRNAscr were incubated with IL-1beta, then a suspension of THP-1 monocytic cells was added to each well. (**c**) Dz13 inhibits inflammation in the mesenteric venules of rats. Fluorescence microscopy on cross sections of mesenteric venules demonstrates FITC-labeled DNAzyme uptake into the venular endothelium. Error bars represent s.e.m. *, $P < 0.05$ compared to control using Student's *t*-test or ANOVA.

monolayers by six- to sevenfold within 30 min (**Fig. 2a**). Prior transfection of endothelial cells with Dz13, unlike Dz13scr, virtually abolished monocytic cell–endothelial adhesion (**Fig. 2a**, upper panel). Similar results were obtained using c-Jun siRNA, but not scrambled siRNA (**Fig. 2b**). In contrast, Dz13 failed to inhibit cytokine-inducible adhesion when the monocytic cells were transfected (**Fig. 2a**, lower panel) despite DNAzyme incorporation in virtually the entire population (**Fig. 2a**, lower panel inset). These findings indicate that Dz13 inhibition of monocytic cell adhesion to cytokine-challenged endothelium relies upon endothelial rather than monocytic cell transfection of DNAzyme.

We next investigated a model of inflammation in the rat mesenteric microcirculation. IL-1beta-induced leukocyte flux (**Fig. 2c**, upper panel), adhesion (**Fig. 2c**, middle panel) and extravasation (**Fig. 2c**, lower panel) in mesenteric venules within 60 min of superfusion. All three processes were completely abrogated by topical delivery of a single dose (35 µg) of Dz13 for 10 min before cytokine exposure, whereas the same amount of Dz13scr had no effect (**Fig. 2c**). Fluorescence microscopy on cross sections of mesenteric venules pretreated with FITC-labeled DNAzyme before IL-1beta administration confirmed DNAzyme uptake into venular endothelium (**Fig. 2c**, right panel).

The multi-staged process of leukocyte trafficking through endothelium is mediated by the dynamic regulation of genes whose products control leukocyte rolling, adhesion and extravasation. These genes are in turn regulated by transcription factors whose expression is exquisitely sensitive to changes in the local humoral milieu. To gain insight into the genes regulated by c-Jun in this process, we performed serial immunohistochemical analysis on DNAzyme-treated mesenteric tissue. Dz13, but not Dz13scr, inhibited c-Jun, E-selectin, vascular cell adhesion molecule (VCAM-1), intercellular adhesion molecule-1 (ICAM-1) and VE-cadherin expression in venule endothelium (**Fig. 3a** and **Supplementary Table 1**), whereas junctional adhesion molecule-1 (JAM-1), platelet-endothelial cell adhesion molecule-1 (PECAM-1) and c-Fos levels were unaffected (**Fig. 3a** and **Supplementary Table 1**). E-selectin mediates leukocyte rolling across

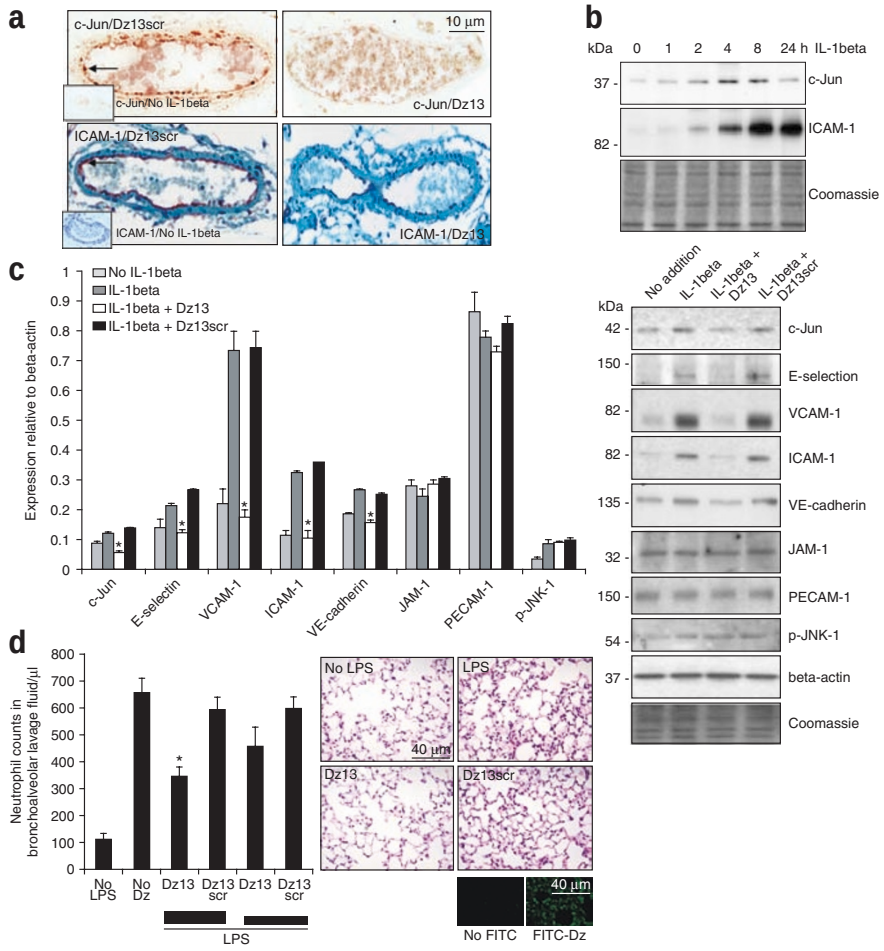

Figure 3 Dz13 inhibits gene expression in mesenteric venular endothelium and microvascular endothelial cells. (**a**) Immunohistochemical analysis was performed for a variety of antigens in rat mesenteric venules (see **Supplementary Table 1** for blinded scoring data). Figure shows representative immunostaining for c-Jun and ICAM-1 (arrows) at 100× magnification. Hematoxylin counterstaining was omitted in the case of c-Jun to demonstrate predominant nuclear staining. (**b**) Western blot analysis of total extracts of microvascular endothelial cells exposed to 20 ng/ml IL-1beta for the times indicated using antibodies to c-Jun and ICAM-1 (left panel) and with extracts harvested 4 h after cytokine treatment with the antibodies indicated (right panel). Cells were transfected with 0.2 μM of Dz13 or Dz13scr. Coomassie blue gel indicates unbiased loading. (**c**) Scanning densitometric assessment of band intensity from western blot analysis normalized to beta-actin. (**d**) Dz13 inhibits neutrophil infiltration in lungs of LPS-challenged mice. Neutrophils in the bronchoalveolar fluid were resuspended in PBS and counted. The figure also shows representative H&E-stained cross sections of paraffin-embedded lung in the 200-μg DNAzyme and control groups at 100× magnification. Fluorescence microscopy demonstrates FITC-DNAzyme localization in lung tissue. Error bars in **c**,**d** represent s.e.m. *, $P < 0.05$ compared to control using Student's *t*-test or ANOVA.

activated endothelium; VCAM-1 and ICAM-1 facilitate leukocyte engagement; and the junctional molecules PECAM-1, VE-cadherin and JAM-1 regulate vascular permeability and leukocyte transendothelial migration[17]. Dz13 therefore suppressed the expression of molecules involved in all stages of the inflammatory process. E-selectin[18], VCAM-1[19] and ICAM-1[20] are encoded by c-Jun-dependent genes. Although it is not known whether c-Jun directly regulates VE-cadherin transcription, the rodent VE-cadherin promoter contains c-Jun recognition elements.

Western blot analysis revealed that IL-1beta stimulates c-Jun expression in microvascular endothelial cells in a time-dependent manner (**Fig. 3b**, left panel). The inducible expression of c-Jun within 1 h preceded that of ICAM-1, which was not apparent until after 2 h (**Fig. 3b**, left panel). Dz13 inhibited IL-1beta-inducible c-Jun expression (**Fig. 3b**, right panel and **Fig. 3c**), whereas Dz13scr had no effect (**Fig. 3b**, right panel and **Fig. 3c**). The DNAzyme also inhibited cytokine-inducible E-selectin, VCAM-1, ICAM-1 and VE-cadherin expression (**Fig. 3b**, right panel and **Fig. 3c**), but did not affect levels of JAM-1 or PECAM-1 (**Fig. 3b**, right panel and **Fig. 3c**), nor did it influence the phosphorylation of c-Jun N-terminal kinase (JNK)-1, whose activity regulates c-*jun* transcription and c-Jun phosphorylation (**Fig. 3b**, right panel and **Fig. 3c**). These data show that reduction in the inducible expression of these pro-inflammatory genes is mediated through inhibition of c-Jun.

Acute inflammation is a key host response mediated by infiltration of circulating leukocytes, principally neutrophils, from the peripheral blood to eliminate pathogens. We assessed the capacity of Dz13 administered by inhalation to modulate acute inflammation in murine lungs challenged with lipopolysaccharide (LPS). LPS caused a robust increase in neutrophil infiltration in bronchoalveolar lavage fluid 4 h after administration (**Fig. 3d**). Dz13 administered once via the airway localized in cells within the alveolar space and the airways (**Fig. 3d**) and suppressed this septic response compared with Dz13scr or the vehicle alone in a dose-dependent manner (**Fig. 3d**).

Rheumatoid arthritis is a common and debilitating disease characterized by inflammation of the distal diarthroidial joints. Inflammatory cell infiltration and synovial hyperplasia in these joints contribute to gradual degradation of cartilage and bone, resulting in the loss of normal joint function. We evaluated the anti-inflammatory effects of Dz13 in the murine collagen antibody–induced arthritis model, which has compelling parallels with human inflammatory joint disease[21]. Joint inflammation is generated by the systemic administration of a cocktail of four separate collagen monoclonal antibodies together with endotoxin. Dz13 (50 μg) was delivered to the hind paw joint intraarticularly, a clinically used route of corticosteroid administration, 3 d after the induction of arthritis. Dz13 inhibited joint thickness (**Fig. 4a**), neutrophil accumulation into the synovium and neovascularization (**Fig. 4a–c** and **Supplementary Table 2**). Dz13 localized to endothelium and other structures within the joint (**Fig. 4b** and data not shown). Notably, Dz13 also blocked the appearance of multinucleated osteoclast-like cells at the bone surface, and bone erosion (**Fig. 4a–c** and **Supplementary Table 2**). Dz13scr, in contrast, had no effect. Thus, Dz13 suppresses inflammation and bone erosion in this well-established murine model of rheumatoid arthritis. Immunohistochemical analysis revealed that Dz13 inhibited the inducible

expression of its target antigen not only in the joint (**Fig. 4d**), but also in the lung (**Fig. 4d**) and retina (**Fig. 4d**), complementing findings in cytokine-treated mesenteric venules (**Fig. 3a** and **Supplementary Table 1**).

Here we investigated the capacity of a catalytic DNA molecule targeting c-Jun to reduce vascular permeability and inflammation. Dz13 blocked vascular permeability in models of immune complex–triggered passive cutaneous anaphylaxis and $VEGF_{165}$-induced leakiness, establishing that c-Jun mediates increased microvascular permeability. Dz13 and an siRNA targeting c-Jun also inhibited retinal neovascularization. Dz13 blocked leukocyte rolling, adhesion and extravasation in the mesenteric venules of rats challenged with IL-1beta. Serial immunohistochemistry and western blot analysis demonstrated that c-Jun is a master regulator of multiple key pro-inflammatory endothelial genes controlling leukocyte trafficking. Dz13 inhibited the expression of E-selectin, VCAM-1, ICAM-1 and VE-cadherin, genes that regulate leukocyte rolling, adhesion and extravasation[22]. Dz13 suppressed neutrophil infiltration in the airways of mice challenged with LPS in a well-established model of lung sepsis. It also inhibited synovial neutrophil infiltration in the collagen antibody–induced arthritis model. Our data therefore indicate that vascular permeability, inflammation and neovascularization are critically dependent upon c-Jun. In all systems, Dz13 efficacy was evaluated alongside its scrambled-arm counterpart, Dz13scr,

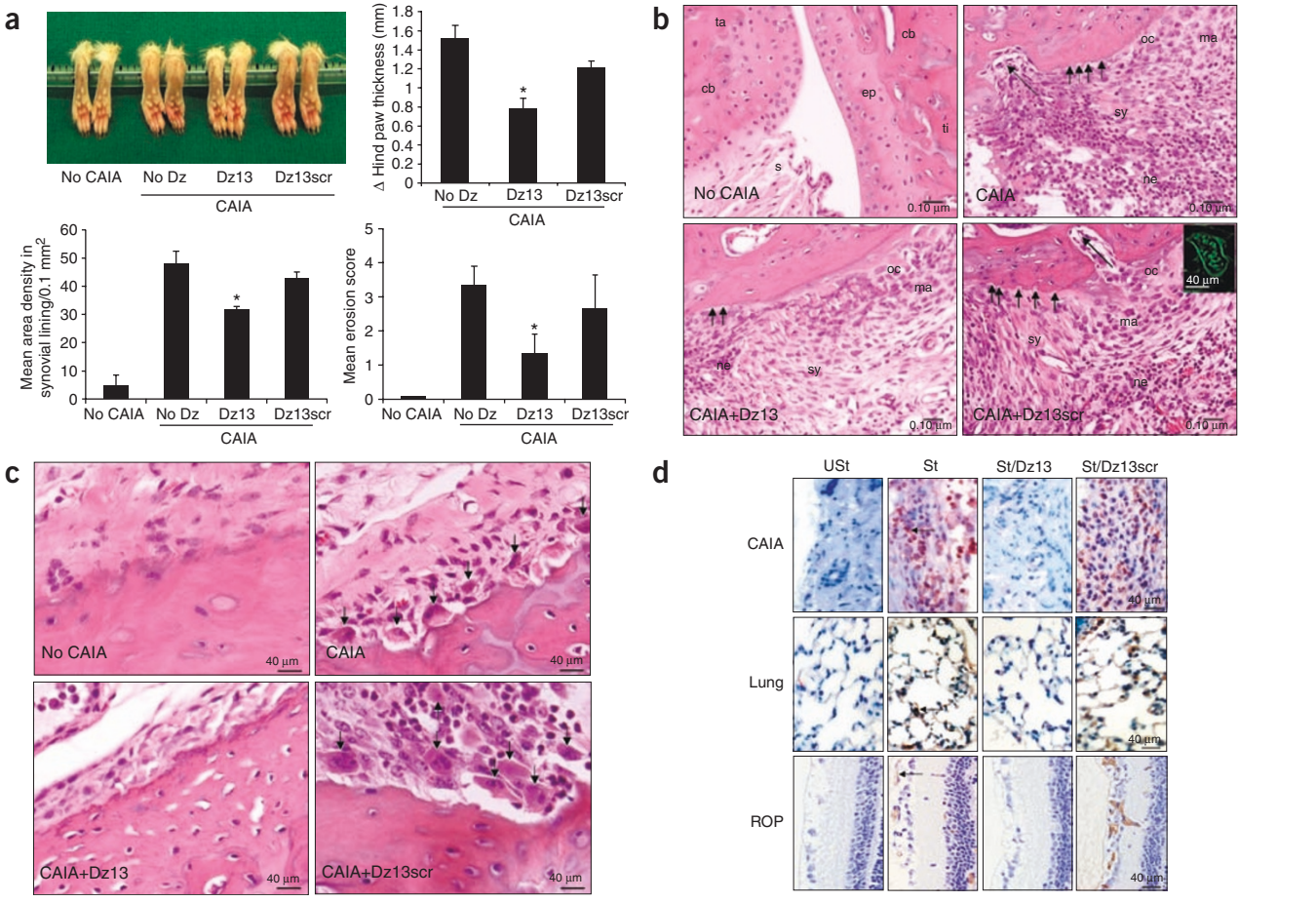

Figure 4 Dz13 inhibits joint thickness and synovial inflammatory cell infiltration in arthritic mice. (**a**) DNAzyme was administered intraarticularly into the hind paw joint of mice previously injected i.p. with a cocktail of four monoclonal antibodies to type II collagen and LPS. Hind paw thickness was determined using electronic Vernier calipers (panel above right). Quantitative assessment of area densities in the synovial lining of the tibiotarsal joint was performed under 200× magnification and a modified version of US National Institutes of Health Image software. Three random areas of synovial tissue on the medial aspect of the joint were assessed for each animal in a blinded fashion (panel below left). Semiquantitative assessment of bone erosion in the talus and distal tibia was made under 200× magnification and a modified tiered scoring criteria (panel below right). (**b**,**c**) Representative high power fields (400× and 600× magnification in **b** and **c**, respectively) showing proximal talus and distal tibia in control mice (No CAIA, for collagen antibody-induced arthritis) and the medial edge of tibia in the other groups in which collagen antibodies were administered. The talus (ta) and tibia (ti) in No CAIA mice has smooth epiphysis (ep) and cortical bone (cb) surfaces; the synovium (S) is also indicated. However, there is extensive erosion of bone on the surfaces of the distal tibia in the CAIA and CAIA+Dz13scr groups (arrows), but not in Dz13 animals. There are substantial differences in the inflammatory cell composition in synovial tissue between the treatment groups. Short and long arrows in **b** indicate modest and severe bone erosion, respectively. Fluorescence microscopy demonstrates FITC-DNAzyme localization within endothelium. Arrows in **c** indicate osteoclasts. The majority of cells in the Dz13 group are fibroblast-like synoviocytes (sy) and macrophages (ma) with a limited number of neutrophils (ne) and osteoclasts (oc). In contrast, a significant proportion of cells in the CAIA and CAIA+Dz13scr groups are neutrophils, with substantial infiltration by macrophages and osteoclasts but limited synoviocites. (**d**) Immunohistochemical analysis for c-Jun antigenicity in Dz13-treated joint (CAIA), lung sepsis and eye (ROP) models. St denotes stimulation (that is, hyperoxia/normoxia, collagen antibodies/LPS or LPS, respectively). Arrows indicate c-Jun antigenicity. Error bars represent s.e.m. *, $P < 0.05$ compared to control using Student's *t*-test or ANOVA.

demonstrating c-Jun sequence specificity. In addition, neither c-Fos, a key partner transcription factor of c-Jun, nor the activated form of its immediate upstream kinase, c-Jun N-terminal kinase-1 (phospho-JNK-1), were affected by Dz13 (**Fig. 3b**,**c** and **Supplementary Table 1**). Dz13 specificity was also demonstrated in ref. 13. This study demonstrates comparable inhibition by Dz13 and a c-Jun siRNA, each targeting different sites in c-Jun mRNA, and shows that Dz13 retains its ability to cleave its target sequence after *in vivo* delivery. The ubiquity of inflammation in a diverse range of human pathologic processes, such as rheumatoid arthritis, asthma, post-infection sepsis, atherosclerotic plaque rupture and erosion, stroke and acute traumatic brain injury, indicates the potential clinical utility of c-Jun-specific interventions as primary inhibitors over steroid-sparing agents or adjuncts.

The '10-23' (ref. 23) type synthetic DNAzymes used in this study contained native phosphodiester linkages rather than phosphorothioates to reduce the propensity for sequence-independent inhibition via nonspecific charge effects. DNAzymes have prima-facie advantages over RNA-based agents and proteins (such as the RNA aptamer pegaptanib (Macugen)[24,25], antibody approaches such as rhuFab[26] and the VEGF receptor ribozyme[27,28]), including lower cost of synthesis, minimal modification, smaller size, target site flexibility and greater stability. That nasally administered siRNA offers protection from respiratory viral infection[29] supports our demonstration of Dz13 delivery via this route. Furthermore, local DNAzyme administration, such as via the intraarticular route used here, is a means of achieving high drug concentrations in the target site while reducing the likelihood of systemic inadvertent side effects. Improvements in DNAzyme technology, such as locked nucleic acid and other modifications[30,31], should further enhance the efficacy of this class of agent.

METHODS

Murine model of proliferative retinopathy. Postnatal day 6 (P6) C57BL/6 mice were exposed to hyperoxia (75% oxygen) for 4 d in Quantum-Air Maxi-Sealed cages. After hyperoxic exposure, P10 mice were returned to normoxia, anaesthetized (17 mg/kg ketamine and 2.5 mg/kg xylazine) and a bolus intravitreal injection of 20 μg of the DNAzyme Dz13, 5′-CGGGAGGAAGGC TAGCTACAACGAGAGGCGTTG (3′-3′ T)-3′; Dz13scr, 5′-GCGACGTGAGGC TAGCTACAACGAGTGGAGGAG (3′-3′ T)-3′ or siRNA (c-Jun siRNA, 5′-r(CAGCUUCCUGCCUUUGUAA)d(TT)-3′; c-Jun siRNAscr, 5′-r(GAUUA CUAGCCGUCUUCCU)d(TT)-3′ in 2 μl saline containing 0.2 μl FuGENE6 (n = 6–12 eyes per group) was administered using a 26-gauge beveled needle attached to a micro-volume syringe (SGE International). The mice were left at room oxygen for a further 7 d before P17 pup eyes were enucleated and fixed in 10% formalin in PBS. Serial 6-μm cross sections of whole eyes were cut sagitally, parallel to the optic nerve, and stained with H&E. Blood vessels from each group were quantified under light microscopy and expressed as the mean ± s.e.m.

Passive cutaneous anaphylaxis. Female six week-old Balb/c mice were injected with 25-ng mouse monoclonal anti-DNP IgE (Sigma) in PBS, pH 7.4, in one ear or with PBS in the other ear. Where indicated, mouse anti-DNP IgE in saline was co-administered with 100 μg DNAzyme (Dz13 or Dz13scr; Tri-Link, synthesized with 3′-3′ linked inverted T) or scrambled DNAzyme in 25 μl of vehicle (FuGENE6 (Roche Diagnostics) in PBS (3:20, vol/vol) containing 1 mM $MgCl_2$) in one ear and the same volume of vehicle in the other ear. After 20 h, mice were injected intravenously with 100 μl PBS containing 100 μg DNP–human serum albumin and 1% Evans blue dye (Sigma). Mice were killed 30 min later and a 6-mm disk biopsy of the ear was obtained with the injection site as the epicenter. Each disc was incubated in 200 μl 10% formamide at 55 °C for 6 h. Dye extravasation was quantified at 610 nm, blanked with formamide. Values were corrected for background absorbance using an untreated patch of skin of identical size.

Miles assay. Anaesthetized 6-week-old female nude Balb/c mice (17 mg/kg ketamine and 2.5 mg/kg xylazine) were injected with 150 μl 1% Evans blue solution into the tail vein. After 5 min, DNAzyme or scrambled DNAzyme in 20 μl vehicle or vehicle alone was delivered into the mid-dorsum by intradermal injection. After 1 h, 50 ng $VEGF_{165}$ (Sigma) in 20 μl PBS was injected into an adjacent location 1 mm away. Extravasation of Evans blue was determined after 90 min by carefully excising the skin around the injection site, incubating in 200 μl 10% formamide for 24 h at 55 °C and measuring optical density at 610 nm. As a negative control, 50 ng of BSA in 20 μl PBS was used. Absorbance at 610 nm was measured as described above.

DNAzyme extraction from injected skin and assessment of cleavage activity. Anaesthetized female 6-week-old Balb/c nude mice were injected intradermally into the mid-dorsum with 100 μg of Dz13. Skin was excised around the injection site after 5 and 60 min and placed in Lysing Matrix D homogenizing tubes (Q-BIOgene) containing 1.2 ml TRIzol (Invitrogen). Tissue was homogenized in a Fast Prep FP120 Bio 101 (Thermo Savant) for 3 cycles at 20 s/cycle. DNA was extracted according to the TRIzol protocol for DNA isolation and purified using P30 micro bio-spin columns (Bio Rad). Synthetic RNA substrate (0.5 μg) was ^{32}P-labeled using T4 polynucleotide kinase and purified from unincorporated nucleotides using P30 micro bio spin columns. Two microliters of DNA isolated from tissue was incubated with 1 μl of labeled RNA substrate for 1 h at 37 °C. Two microliters of the cleavage reaction was added to 4 ml of formamide loading dye and loaded onto a 12% denaturing PAGE gel. Cleavage products were visualized by autoradiography.

Endothelial-monocytic cell adhesion assay. Human microvascular endothelial cells (HMEC-1) grown in 24-well plates at 80–90% confluence were transfected with 0.05 μM of the DNAzyme or siRNA (using FuGENE6) after changing the growth medium from 10% serum to serum free. After 18 h, the cells were washed with PBS and fresh serum-free medium containing 20 ng/ml of IL-1beta was added. After 12 h, THP-1 monocytic cells were added to each well at density of 2.5×10^5 cells per well. Alternatively, the THP-1 cells were transfected with 0.05 μM of Dz13 or Dz13scr and, after 18 h added to cytokine-treated endothelial cultures in 24-well plates at a density of 2.5×10^5 cells per well. After 30 min, the wells were washed thrice with PBS to remove nonadherent cells. Monocytic cells adherent to endothelium were counted as the number of translucent cells per visual field using the 100× objective of a phase-contrast Olympus microscope.

Rat peritoneal mesenteric venule inflammation. Male Sprague-Dawley rats (230–300 g) were anaesthetized with sodium thiobutabarbital (Inactin, 100 mg/kg injected intraperitoneally (i.p.)) and a tracheostomy performed for airway management throughout the experiment. A catheter was inserted into the right femoral artery for intravenous saline administration and blood pressure monitoring. After midline abdominal incision, part of the mesentery from the small bowel was exteriorized and placed on a temperature-controlled Plexiglass chamber for observation of the mesenteric microcirculation using intravital microscopy. The small bowel and mesentery were continuously superfused with modified Krebs-Henseleit solution at 37 °C. Mesenteric venules of 25–50 μm diameter and >100 μm length were selected. Images from an Olympus microscope were projected by a high-resolution color video camera (JVC) into a color high-resolution video-monitor and recorded on Super-VHS tapes. All images were analyzed offline for three parameters of inflammation: leukocyte flux, adhesion and extravasation. Rolling leukocyte flux was measured by counting cells rolling past a defined reference point within the 100-μm vessel length per min. Leukocyte adhesion was assessed by counting leukocytes that remained stationary for at least 30 s per 100 μm of length of vessel. Leukocyte numbers in tissue adjacent to the venule per microscopic field were used to quantify extravasation. Venules were monitored for baseline flux, adhesion and extravasation 20–30 min before the commencement of each treatment. One hundred μl of either vehicle or vehicle containing DNAzyme (35 μg) was applied topically and left undisturbed for 10 min during which time superfusion was temporarily stopped to facilitate DNAzyme infusion. Superfusion was resumed with either modified Krebs-Henseleit buffer or buffer containing IL-1beta (20 ng/ml). Video recordings for each treatment

were made at the time of application of vehicle or vehicle plus DNAzyme and 60 min after application. The following exclusion criteria were used before addition of vehicle or IL-1: leukocyte flux >35 cells/min; >3 adherent cells per 100 μm of vessel; >10 extravasated leukocytes in the field of view after 20 min of undisturbed superfusion. Leukocyte flux, adhesion and extravasation were quantified offline at the conclusion of the experiment.

Western blot and immunohistochemical analysis. Western blot analysis was performed essentially as previously described using commercialrabbit or goat anti-peptide polyclonal antibodies to c-Jun, E-selectin, VCAM-1, ICAM-1, VE-cadherin, JAM-1, PECAM-1, p-JNK-1 and beta-actin (Santa Cruz Biotechnology, R&D Systems, Alexis Biochemicals). Immunostaining was performed on formalin-fixed, paraffin-embedded mesenteric tissue with rabbit or goat polyclonal antipeptide antibodies essentially as described[15].

LPS-induced pulmonary infiltration. DNAzyme (100 μg or 200 μg/50 μl) was administered into the lung via the nares of 7- to 8-week-old Balb/c mice 2 h before LPS (Difco, *Escherichia coli*) delivery (10 μg/40 μl). Control mice received 40 μl vehicle. Four hours after LPS administration, mice were killed with an overdose of ketamine and xylazine (500 mg/kg and 50 mg/kg, respectively). Lungs were perfused by cardiac puncture via the right ventricle with saline then a tracheostomy performed with an 18-gauge needle. Bronchoalveolar lavage fluid was obtained by washing the lungs three times with 1 ml Hank's balanced salts solution. Cells were pelleted at 400*g* for 5 min then resuspended in 200 μl of PBS. Neutrophils were counted using a hemocytometer and expressed as cell counts/μl.

Collagen antibody-induced arthritis Arthritis was induced in 6-week-old Balb/c mice by injection i.p. of a commercially obtained (Chemicon International) cocktail of four monoclonal antibodies to type II collagen (2 mg/mouse) followed by a second injection i.p. 72 h later of 50 μg LPS[32]. DNAzyme (50 μg/5 μl) was administered directly (intra-articular route) into hind paw joint at the time of the second injection. After 9 d, the mice were killed by cervical dislocation and hind paw thickness was determined using electronic Vernier calipers. Hind limbs were fixed in 10% formalin in PBS, decalcified in 30% formic acid and 10% formaldehyde in water for 24 h, their heels removed and processed into paraffin. Sagittal sections across the heel, 4- to 7-μm thick, were stained with standard H&E. The degree of inflammation in the synovial lining was evaluated by analyzing the mean density of three randomly selected (using MS Excel) areas (0.1 mm^2) in the medial aspect of the tibiotarsal joint under 200× magnification using an Olympus BX60 microscope and a modified version of NIH Image software (ImageJ software, Wright Cell Imaging Facility, Toronto Western Research Institute). The relative proportions of polymorphonuclear and mononuclear cells in each section was evaluated by counting 3 × 100 cells in two to three adjacent high power fields (400× magnification) at the bone-synovial tissue junction. To grade bone erosion, we evaluated paw sections using a modified semiquantitative scoring criteria previously described[33]. In brief, bone erosion score 0 represents normal bone integrity; 1, minimal loss of cortical or trabecular bone; 2, moderate loss of bone at the edges of talus and minimum loss in cortex of distal tibia; 3, marked loss of bone at the edges of talus and moderate loss in the cortex of distal tibia; 4, marked loss of bone in both talus and tibia. For consistency, scoring was performed on the talus and tibia under 200× magnification.

DNAzyme localization studies. We injected 20 μg of FITC-DNAzyme (TriLink-BioTechnologies) intraarticularly (CAIA model), intradermally (Miles or PCA assay) or intravitreally (ROP model) into anaesthetized (17 mg/kg ketamine, 2.5 mg/kg xylazine) female 6-week-old Balb/c, Balb/C nude or C57BL/6 mice respectively. In the lung model, 20 μg of the FITC-DNAzyme was delivered by inhalation to female 6-week-old Balb/c mice. Areas of tissue localization were removed from overanaesthetized mice (100 mg/kg ketamine, 5 mg/kg xylazine) and visualized by fluoroscopy at 400× magnification.

Animal ethics and statistical analysis. All animal experiments were approved by the Animal Care and Ethics Committee, The University of New South Wales, and purchased from the Biological Resources Centre, University of New South Wales. All values are expressed as the mean ± s.e.m. Differences between groups were tested for statistical significance using Student's *t*-test or analysis of variance (ANOVA). Differences were considered to be significant at $P < 0.05$.

Note: Supplementary information is available on the Nature Biotechnology website.

ACKNOWLEDGMENTS

We thank Nick diGirolamo for his expertise in immunohistochemistry, and Ravinay Bhindi and Akiko Maekawa for their assistance with intra-articular and tail vein injections, respectively. This work was supported by grants from the NHMRC, NHF, Diabetes Australia, Cancer Council, Johnson & Johnson Research Pty Limited and the NSW Department of Health. L.M.K. is a Senior Principal Research Fellow of the NHMRC.

AUTHOR CONTRIBUTIONS

All authors contributed intellectually and/or technically to this project. L.M.K. conceived, designed and supervised all aspects of the project.

COMPETING INTERESTS STATEMENT

The authors declare that they have no competing financial interests.

Published online at http://www.nature.com/naturebiotechnology/
Reprints and permissions information is available online at http://npg.nature.com/reprintsandpermissions/

1. Davies, N.M. Review article: non-steroidal anti-inflammatory drug-induced gastrointestinal permeability. *Aliment. Pharmacol. Ther.* **12**, 303–320 (1998).
2. Botting, R. Antipyretic therapy. *Front. Biosci.* **9**, 956–966 (2004).
3. Howard, P.A. & Delafontaine, P. Nonsteroidal anti-Inflammatory drugs and cardiovascular risk. *J. Am. Coll. Cardiol.* **43**, 519–525 (2004).
4. Schuff, K.G. Issues in the diagnosis of Cushing's syndrome for the primary care physician. *Prim. Care* **30**, 791–799 (2003).
5. Cirino, G., Fiorucci, S. & Sessa, W.C. Endothelial nitric oxide synthase: the Cinderella of inflammation? *Trends Pharmacol. Sci.* **24**, 91–95 (2003).
6. Carmeliet, P. Angiogenesis in health and disease. *Nat. Med.* **9**, 653–660 (2003).
7. Murohara, T. *et al.* Vascular endothelial growth factor/vascular permeability factor enhances vascular permeability via nitric oxide and prostacyclin. *Circulation* **97**, 99–107 (1998).
8. Gamble, J.R. *et al.* Angiopoietin-1 is an antipermeability and anti-inflammatory agent in vitro and targets cell junctions. *Circ. Res.* **87**, 603–607 (2000).
9. Ito, Y. *et al.* Inhibition of angiogenesis and vascular leakiness by angiopoietin-related protein 4. *Cancer Res.* **63**, 6651–6657 (2003).
10. Chen, J. *et al.* Akt1 regulates pathological angiogenesis, vascular maturation and permeability *in vivo*. *Nat. Med.* **11**, 1188–1196 (2005).
11. Santiago, F.S. *et al.* New DNA enzyme targeting Egr-1 mRNA inhibits vascular smooth muscle proliferation and regrowth factor injury. *Nat. Med.* **5**, 1264–1269 (1999).
12. Lowe, H.C., Chesterman, C.N. & Khachigian, L.M. Catalytic antisense DNA molecules targeting Egr-1 inhibit neointima formation following permanent ligation of rat common cartoid arteries. *Thromb. Haemost.* **87**, 134–140 (2002).
13. Khachigian, L.M., Fahmy, R.G., Zhang, G., Bobryshev, Y.V. & Kaniaros, A. c-Jun regulates vascular smooth muscle cell growth and neointima formation after arterial injury: inhibition by a novel DNAzyme targeting c-Jun. *J. Biol. Chem.* **277**, 22985–22991 (2002).
14. Lowe, H.C. *et al.* Catalytic oligodeoxynucleotides define a key regulatory role for early growth response factor-1 in the porcine model of coronary in-stent restenosis. *Circ. Res.* **89**, 670–677 (2001).
15. Zhang, G. *et al.* Effect of deoxyribozymes targeting c-Jun on solid tumor growth and angiogenesis in rodents. *J. Natl. Cancer Inst.* **96**, 683–696 (2004).
16. Smith, L.E. *et al.* Oxygen-induced retinopathy in the mouse. *Invest. Ophthalmol. Vis. Sci.* **35**, 101–111 (1994).
17. Engelhardt, B. & Wolburg, H. Transendothelial migration of leukocytes: through the front door or around the side of the house? *Eur. J. Immunol.* **34**, 2955–2963 (2004).
18. Min, W. & Pober, J.S. TNF initiates E-selectin transcription in human endothelial cells through parallel TRAF-NF-kappa B and TRAF-RAC/CDC42-JNK-c-Jun/ATF2 pathways. *J. Immunol.* **159**, 3508–3518 (1997).
19. Ahmad, M., Theofanidis, P. & Medford, R.M. Role of activating protein-1 in the regulation of the vascular cell adhesion molecule-1 gene expression by tumor necrosis factor-alpha. *J. Biol. Chem.* **273**, 4616–4621 (1998).
20. Wang, N. *et al.* Adenovirus-mediated overexpression of c-Jun and c-Fos induces intercellular adhesion molecule-1 and monocyte chemoattractant protein-1 in human endothelial cells. *Arterioscler. Thromb. Vasc. Biol.* **19**, 2078–2084 (1999).
21. Staines, N.A. & Wooley, P.H. Collagen arthritis–what can it teach us? *Br. J. Rheumatol.* **33**, 798–807 (1994).
22. van Buul, J.D. & Hordijk, P.L. Signaling in leukocyte transendothelial migration. *Arterioscler. Thromb. Vasc. Biol.* **24**, 824–833 (2004).
23. Santoro, S.W. & Joyce, G.F. A general purpose RNA-cleaving DNA enzyme. *Proc. Natl. Acad. Sci. USA* **94**, 4262–4266 (1997).

24. Eyetech Study Group. Preclinical and phase 1A clinical evaluation of an anti-VEGF pegylated aptamer (EYE001) for the treatment of exudative age-related macular degeneration. *Retina* **22**, 143–152 (2002).
25. Gragoudas, E.S., Adamis, A.P., Cunningham, E.T., Jr., Feinsod, M. & Guyer, D.R. Pegaptanib for neovascular age-related macular degeneration. *N. Engl. J. Med.* **351**, 2805–2816 (2004).
26. Ferrara, N. Role of vascular endothelial growth factor in physiologic and pathologic angiogenesis: therapeutic implications. *Semin. Oncol.* **29**, 10–14 (2002).
27. Parry, T.J. *et al.* Bioactivity of anti-angiogenic ribozymes targeting Flt-1 and KDR mRNA. *Nucleic Acids Res.* **27**, 2569–2577 (1999).
28. Pavco, P.A. *et al.* Antitumor and antimetastatic activity of ribozymes targeting the messenger RNA of vascular endothelial growth factor receptors. *Clin. Cancer Res.* **6**, 2094–2103 (2000).
29. Bitko, V., Musiyenko, A., Shulyayeva, O. & Barik, S. Inhibition of respiratory viruses by nasally administered siRNA. *Nat. Med.* **11**, 50–55 (2004).
30. Fahmy, R.G. & Khachigian, L.M. Locked nucleic acid-modified DNA enzymes targeting early growth response-1 inhibit vascular smooth muscle cell growth. *Nucleic Acids Res.* **32**, 2281–2285 (2004).
31. Breaker, R.R. Natural and engineered nucleic acids as tools to explore biology. *Nature* **432**, 838–845 (2004).
32. Kagari, T., Doi, H. & Shimozato, T. The importance of IL-1 beta and TNF-alpha, and the noninvolvement of IL-6, in the development of monoclonal antibody-induced arthritis. *J. Immunol.* **169**, 1459–1466 (2002).
33. Bolon, B., Morony, S., Cheng, Y., Hu, Y.L. & Feige, U. Osteoclast numbers in Lewis rats with adjuvant-induced arthritis: identification of preferred sites and parameters for rapid quantitative analysis. *Vet. Pathol.* **41**, 30–36 (2004).

Corrigendum: Suppression of vascular permeability and inflammation by targeting of the transcription factor c-Jun

Roger G Fahmy, Alla Waldman, Guishui Zhang, Ainslie Mitchell, Nicodemus Tedla, Hong Cai, Carolyn R Geczy, Colin N Chesterman, Michael Perry & Levon M Khachigian

***Nat. Biotechnol.* 24, 856–863 (2006); published online 2 July 2006; corrected after print 10 June 2015**

In the version of this article initially published, the first three bars in the histogram in Figure 1a should have read "No vehicle," "No Dz" and "Dz13" instead of "No Dz," "Dz13" and "Dz13scr." The legend of Figure 1a should have included the sentences: "'No vehicle' represents the normoxia control without vehicle (transfection agent) or DNAzyme or siRNA. All other groups contain vehicle." The H&E-stained images in Figure 1a should have read "Dz13 in hyperoxia-normoxia" and "Dz13scr in hyperoxia-normoxia" instead of "Normoxia" and "Hyperoxia-normoxia." None of the conclusions is affected by the errors. The errors have been corrected in the HTML and PDF versions of the article.